THE CLUSTERIZATION ALGORITHMS IN MULTIFRAGMENTATION

A thesis submitted in the partial fulfillment of requirement for the award degree of

Masters of Science

In

Physics

Submitted by

Ekta Bansal

Roll No.-300804007

Under the esteemed guidance of

Dr. Suneel Kumar

(Assistant Professor)

School of Physics and Materials Science

Thapar University

PATIALA (PUNJAB)-147004

July 2010

CERTIFICATE

This is to certify that Ms. Ekta, Roll No. 300804007 has worked on this thesis report as a partial fulfillment for award of the degree of **MASTERS OF SCIENCE** in physics. I certify that the matter embodied in this report is of candidate's own record and not submitted to any other university in any part or full form for the award of such a degree.

S Kumar

Ekta
(Ekta)

(Dr. Suneel Kumar)
Assistant Professor ***(Supervisor)***
SPMS, Thapar University
Patiala.

Countersigned by:

Dr. O.P. Pandey
(Prof. & Head)
SPMS
Thapar University,
Patiala.

23/7/1

Dr. R.K. Sharma
Dean of Academic Affairs
Thapar University,
Patiala.

Acknowledgement

I owe my deepest gratitude to **Dr. Suneel Kumar**, *my worthy supervisor*, who has been an inspiration during my research work. Without him, this thesis would not have been possible. I thank him for his patience and encouragement that carried me on through difficult times, and for his insights and suggestions that helped to shape my research skills. I express my sincere thanks to him for his valuable guidance in carrying out work under his effective supervision, encouragement and cooperation. His visionary thoughts have influenced me greatly. His dynamical attitude has empowered me with zeal of energy to conquer the minor details of my research work.

I also thank **Dr. O. P. Pandey**, Professor and Head, School of Physics and Material Science for his support and providing facilities.

A special word of thanks to **Mr. Sanjeev Kumar and Mrs. Varinderjit Kaur**, Research Scholars for the help and valuable suggestions whenever I needed out of their busy schedule.

Special thanks are due to all my friends Ruhi, Bahadur, Mandeep, Dolly, Bhawana Ritu and Charu and the staffs at the School of Physics and Material Sciences for providing me a friendly atmosphere and encouraging me throughout this work.

I am deeply thankful to my Family, their moral support and patience has bared fruit through completion of this Thesis.

Ekta

Roll No: 300804007

DEDICATED

TO

MY FAMILY…

Abstract

In the present thesis, we analyze the formation of fragments in two different reactions at different incident energies $^{129}Xe_{54}+^{197}Au_{79}$ at E=50MeV/nucleon and $^{36}Ar_{18}+^{197}Au_{79}$ at E=50, 80,110MeV/nucleon at different impact parameters using hard and soft equations of state. For the present analysis, Isospin Dependent Quantum Molecular Dynamics Model (IQMD) is used as an event generator. To address the stability of fragments, we employ three different clusterization algorithms methods i.e. Minimum Spanning Tree method (MST), Minimum spanning tree with momentum cut (MSTP) and Minimum Spanning Tree with Binding Energy Check (MSTB). Our analysis shows that the fragment created are not stable even at 100 fm/c and an additional binding energy checks helps to discard the unbound fragments and as result the modified MST (with the binding energy check) identifies the fragments early. The comparison is performed for the free nucleons as a function of impact parameter using hard equation of state with experimental data in two different reactions at different incident energies. The MSTB method can be applied whenever one wants to identify the fragments which are of given number of constituents form bound objects.

Table of Contents Page No.

List of Figures and tables

Chapter 1

Introduction

The nuclear physics (at low/intermediate/high energies) is one of the most extensively studied field. In recent years, a lot of efforts have been made at low, intermediate and relativistic energies to understand the heavy ion reactions. The heavy ion collisions provide unique possibility to understand the different observables and phenomena which emerges at different incident energies and at collision geometries. After many decades, nuclear physics has reached a moment of critical differentiation. It has been differentiated in four branches which are given as:

- Deconfinement and quark gluon plasma
- Low energy γ-ray spectroscopy.
- Nuclear collectivity through giant resonances.
- Compound nucleus and fission studies

1.1 Low, intermediate and high energies

The study of nuclear reactions from low to relativistic energies provides variety of phenomena.

- At low energy, Pauli principle blocks significant scattering of the nucleons. Therefore mean field dominates the physics at low energy.
- At intermediate energy, a mixture of attractive mean field and repulsive nucleon-nucleon scattering exists.
- At high energy, only nucleon-nucleon scattering exists.

It is interested to study the low energy nuclear physics or the heavy ion collision for the low density phenomena. The colliding nuclei at low incident energies cannot compress each other; therefore one has studied the physics of sub-density phenomena. The low

energy heavy-ion reactions ($E_{incident} \leq 20$MeV /nucleon) look for the nuclear interactions as well as fusion-fission, cluster-radioactivity, formation of super heavy nuclei, etc [1]. The low energy physics has been explored by studying variety of experiments which involve both symmetric as well as asymmetric nuclei [1]. The heavy ion collision at intermediate energies (20 MeV/nucleon$\leq E_{incident} \leq$2000MeV /nucleon) produces a piece of hot and dense nuclear matter. In addition, several rare phenomena like the multi-fragmentation, collective flow and sub-threshold particle production are also observed [2]. These parameters can be further understood by the phase diagram of nuclear matter.

1.2 Nuclear phase diagram

Fig 1.1 shows the phase diagram of nuclear matter in temperature-density plane. Like all other materials, the properties of nuclear matter are also influenced by the pressure, density and temperature. The hadron matter (strongly interacting particles) may have rich structure in the domain of high excitation energies and compressions. From fig 1.1 one can see the nuclear liquid-vapor phase transition at low temperature and sub-nucleonic densities. At very high density and temperature, we have quark gluon plasma [3-4] whereas at moderate temperatures, the hadron-gas can occur which can be studied through intermediate energy heavy-ion collisions.

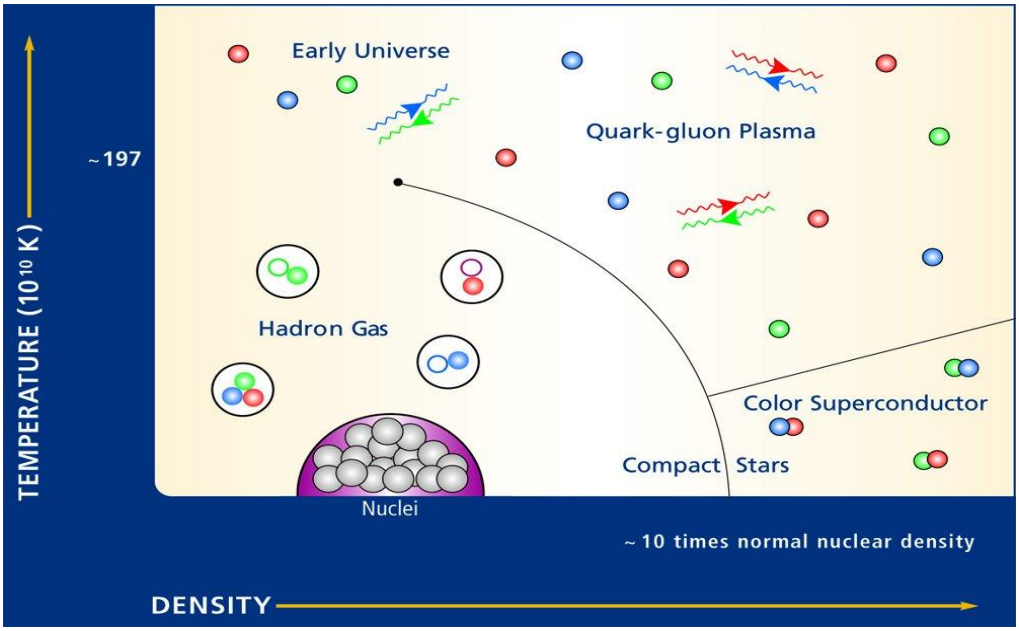

Fig 1.1. Nuclear phase diagram

Let us examine the other possible candidates for higher temperatures and densities. Table 1.1 gives the list of different possible candidates for higher temperatures and densities. Table 1.1 gives the list of different possible candidates that can produce high densities and temperatures. From table1.1, we see that the finite nuclei can generate nuclei with small fluctuations in the density and temperatures.

Candidate	Max. density	Max temp.	Comment
Finite nucleus (monopole)	$\rho/\rho_0 \approx 1$	T≈ 0 MeV	Very small range of density is available
Neutron star	$\rho/\rho_0 \approx 6$	T≈0 MeV	Rare in time and remote in space
supernova	$\rho/\rho_0 \approx 4$	T≈10 MeV	Rare in time and remote in space
Heavy ion collisions intermediate energies	$\rho/\rho_0 \approx 2$-3	T≈100 MeV	Give unique possibility to study the matter at high density and temperature.

Table 1.1 candidates for high densities and temperature

Therefore, these are not to be used to study the matter at the extreme densities and temperatures. The next two candidates namely the neutron star and supernova explosion are remote in space and rare in time, therefore provide a limited possibility to extract the information about the matter at high temperature and density. The last candidate i.e. the heavy- ion collision at intermediate and relativistic energies provides unique possibility to study the properties of hadrons over a wide range of temperature and density [2-3]. In addition, one can also examine the properties of hadrons in medium. Note that the experimental measurements are done at the end of the reaction where matter is cold and well separated. In other words, one cannot study the hot and dense matter directly in experiments. One has to rely on indirect methods to extract the information about the hot and dense matter. It is worth mentioning that the hot and dense matter directly produced

in the collision of heavy nuclei (at intermediate energies) remains for very short span of the time (≈20fm/c) [2-4]. This hot and dense piece of nuclear matter gives rise to various phenomena like the flow of nucleons, sub-threshold particle production, multi-fragmentation, nuclear stopping, directed as well as elliptical flow etc. Since, we are interested in the process of multifragmentation due to availability of experimental data, so multifragmentation is discussed in detail in the following section.

1.3 Multi-fragmentation

It is well known that the colliding nuclei (at intermediate energies) shatter into several small and medium size pieces and lot of nucleons are also emitted. This branch is called multi-fragmentation. One is struggling to find the answer of typical question like why do nuclei break into several fragments? How and when these fragments are formed? How the medium does affects the clusterization? What is the mechanism behind the multi-fragmentation? Why does a nuclei shatter into several fragments, if hit by a projectile? Is this a statistical process or this is a dynamical etc? During the last two decades, extensive efforts have been made experimentally as well as theoretical to find the possible answer of all these questions. The present thesis also deals with multi-fragmentation. We shall attempt to extract the information about several equation of state by comparing our theoretical results of different analysis with experimental data.

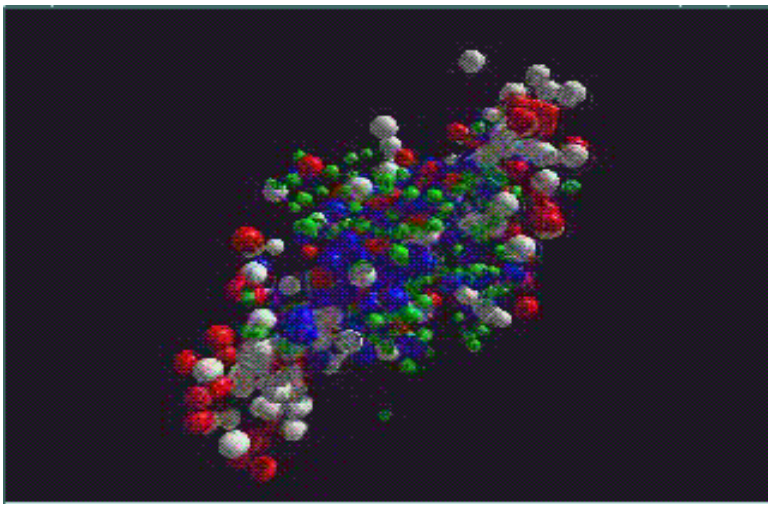

Fig 1.2 Excited nucleus breaks into the various fragments: multifragmentation

In the following, we shall first present a brief survey of experimental status and therefore a brief discussion of various theoretical methods will be made. The detailed discussion on different theoretical tools is given in chapter 2.

1.4 Review of experimental attempts for multifragmentation

Before two decades, it was not possible to accelerate the heavy nuclei and therefore one could accelerate the light ions and particles only. The field of heavy- ion physics was dominated by shooting light particles on heavy targets. In other words, the study of nuclear physics was confined to fusion, fission, particle transfer etc. At present, we are able to accelerate the nuclei up to several hundreds of GeV/ nucleon that have opened new dimensions in the field of intermediate and high energy heavy-ion reactions.

In 1974, the BEVLAC accelerator at Lawerence Berkley Laboratory (LBL) became capable of accelerating heavy nuclei such as iron up to incident energies of 2.1 GeV/ nucleon [2]. This was the beginning of new era in accelerator based heavy- ion physics. Since a piece of hot and compressed nuclear matter can be produced in heavy ion collisions, these experiments were aimed to determine the nuclear equation of state [2].

After the first Berkley experiments, several accelerators were built made at Michigan State University (MSU) USA, GANIL (France) and at GSI is specifically designed to study the heavy-ion collisions at intermediate energies. The experimental group at MSU is very active in studying the fragment spectra at lower side of the bombarding energies. Similar efforts are also made by the INDRA collaboration at GANIL and by the ALADIN/FOPI collaboration at GANIL and by the ALADIN/FOPI collaboration at GSI. These measurements provide complete spectra of fragments over wide range of incident energies and impact parameters which include the fusion, fission, multifragmentation as well as total disassembly of the nuclear matter at higher incident energies.

The INDRA collaboration at GANIL, France [5] is studying the collisions with large nucleonic multiplicities. They have undertaken an ambitious program where influence of different parameters on multi-fragmentation is analyzed. These parameters include the role of system- size in entrance channel as well as in Coulomb instabilities. In addition, system- size are studied in symmetric collisions of ^{36}Ar+KCl(AT 32, 40,52 and 74MeV/nucleon)[6], ^{58}Ni + ^{58}Ni (at 32, 40, 52,63,74,82 and 90 MeV/nucleon. On the other hand, the entrance channel effects are studied by keeping the total mass equal to 250 units. The gentle compression and Coulomb instabilities were studied for heavy fragments.

The Berkley group has concentrated mainly on the asymmetric reactions like ^{197}Au + ^{27} Al, ^{51}V and ^{64}Cu at 60 MeV/nucleon [7] or ^{197}Au + ^{27} Al at 50 MeV/nucleon and 110 MeV/nucleon[6], ^{58}Fe + ^{197} Au at 50MeV/nucleon and 100 MeV/nucleon[7] etc. they concentrated on different probabilities which include the excitation energy, angular distribution and velocity distribution etc.

The FOPI and ALADIN groups at GSI are studying variety of reactions with all kind of possibilities. It ranges from ^{12}C to ^{208} Pb and with incident energy between 100 MeV/nucleon and 1000 MeV/nucleon [8]. A lot of physical conclusions are also drawn from these studies. The ALADIN group [9] reported a target independence above 600 MeV/nucleon if fragment multiplicities are plotted against Z_{bound} (=sum of the charges of all fragments with $Z \geq 2$). This is valid if incident energy is above 600 MeV/nucleon and projectile is kept fixed. For different projectile, one has to rescale the quantities charge of target with the charge of projectile. These experiments also established the relation between the impact parameter and emission of projectile. A larger multiplicity indicates the central collision decrease with increase in the impact parameter. Besides from these observations, the properties of fragments like collective flow, energy spectra, rapidity distribution are also investigated [9]. The nucleons are found to be emitted from participant zone whereas the heavy fragments are the remnants of spectators. The collective flow is found to increase with increase n the size of fragments. In other words, the fragments are found to exhibit a larger flow compared to nucleons.

1.5 Review of theoretical models for multi-fragmentation

Before looking for theoretical models and algorithms suitable at intermediate and relativistic energies, we have to keep in mind the dynamics involved at these energies. At low incident energy, the possibility of nucleon-nucleon collision and nucleonic degree of freedom is very small; therefore, nuclear dynamics can be understood by studying the real part of the potential only. On the other hand, the frequent nucleon- nucleon collisions relativistic energies need imaginary part of the potential (which is proportional to the nucleon-nucleon cross section). At intermediate energy, both real and imaginary parts of the potential are comparable. Two different assumptions had been given to understand the dynamics at intermediate energies.

(1). One assumes the final state of the reaction is decided by the statistical methods. These methods are widely used to understand various observables. The crucial input in these models is the excitation energy and density of the system at freeze-out time. In earlier calculations, one has assumed these parameters, whereas recent calculations have been done with phase space generated by dynamical models [10].

(2). The second assumption was final state of reaction is decided by dynamical methods. It starts with two nuclei and follows the dynamics of the collision with dynamical models. These models are capable of studying the detailed reaction with many body features. As our present interest is to understand the formation of fragments, we shall study the dynamics of formation of fragments using IQMD model. The phase space is obtained by IQMD will be analyzed by different clusterization algorithms like MST and MSTB and then will compare with experimental findings [11].

A nucleus- nucleus collision at intermediate energy can be viewed as composed of three stages [2, 3] which are given as following:

(1). The first is the initial stage where the target and projectile are prepared and boosted towards each other with proper centre of mass energy.

(2). In the second stage, reaction happens and matter is compressed and obtain a piece of hot and dense nuclear matter. This is called compressional stage.

(3). The compressed and hot nuclear matter expands to sub-nucleonic densities which will break the matter into large number of entities consisting of emitted nucleons as well as light and medium mass fragments. The size and multiplicity of various fragments depends crucially on the incident energy as well as on the impact parameter of the reaction which will be discussed in chapter 3.

It has been mentioned that all dynamical models follows the evolution of single nucleons only. No dynamical model simulates the clusters production directly. Therefore, we need algorithms to identify the clusters. In other words, the study of multi-fragmentation can be divided into two parts:

(1). The calculations of phase space of nucleons.

(2).The clusterization of the calculated phase space using cluster recognition algorithms.

Theoretically, several models have been developed which make the situation more complicated. The key point to remember is that heavy-ion collision involves very complicated non-equilibrium physics; therefore, its numerical modeling is not straight forward. Due to lack of free space at low incident energies about 96% of the attempted collisions are blocked. The whole dynamics at low energies is governed by the mean field or by the two body and three body interactions. In contrary the availability of large free phase space at relativistic energies (>2 GeV/nucleon) makes Pauli Principle role quite small (roughly 4% collisions are blocked) and hence the dynamics of reaction is governed by the Cascade picture. These conditions are satisfied by Classical Molecular Dynamics (CMD) which is further modified for the Quantum features.

1.6 Primary Models

Molecular dynamics: The classical molecular dynamics (MD) [12] approach is capable of treating both compression and fragment formation. The molecular dynamics predicts the collective flow in a qualitative agreement with the data. It incorporates the complete classical N-body dynamics which is necessary to describe the formation of

fragments. Naturally, the simple classical molecular dynamics needs refinement which should also include quantum features. In nuclear physics, the key problem in MD methods lies in the treatment of the Pauli Principle. Nucleons are fermions and it is difficult to speak of nuclei without the Pauli Principle. This question is simply overlooked in strictly classical calculations. MD methods with Pauli principle address this question but with disputable success.

Quantum Molecular Dynamics: The QMD model [13] attempts to manipulate a many-body wave function to introduce the correlations needed for cluster formation. Taking the wave function as a product of coherent states with Pauli blocking, the model evolves a set of test particles through the temporal evolution of the reaction.

In past decade, several refinements and improvements were made over original QMD. The Quantum Molecular Model (QMD) model takes into account the Pauli principle, but through two-body collisions, which is somewhat contrary to Molecular Dynamics (MD) picture. In view of the difficulties encountered with taking the Pauli principle in classical MD methods properly into account, a new class of approaches was developed in the beginning of the 1990s, the so called Fermionic Molecular Dynamics (FMD) [14] and for Antisymmerized Molecular Dynamics (AMD) [15,16]. The serious numerical problems have restricted the use of FMD and AMD approaches to light nuclei. The new versions were named as IQMD (Isospin-QMD), GQMD (G-matrix-QMD) [17]. It is worth to mention that the Intra nuclear Cascade model (INC) developed by Cugnon *et. al* [18], is one of the pioneering models in the field and has acted as a guideline for the development of the field. Recently, IQMD Model has been attracted the scientific community due to the different behavior of neutron and protons at intermediate energies.

Isospin dependent Quantum Molecular Dynamics: IQMD model [19] in heavy ion collisions is used for studying the isospin effects on nuclear transverse collective flow, on nuclear radial flow and nuclear fragmentation. The dynamics in the formation of the transient state is mainly governed by three components namely, mean field, two body

collisions, and Pauli blocking. For an isospin dependent reaction dynamics, it is essential that all the three components should reasonably include isospin degrees of freedom. In addition, it is also important that, in initialization of projectile and target nuclei, the samples of neutrons and protons in phase space should be treated separately since there exists a large difference between neutron and proton density distributions for nuclei. IQMD model is developed just on above basis. It has been shown that the IQMD can be used with large success for studying the effects of isospin in heavy ion collisions at intermediate energies.

1.7 Secondary Models

Cluster Analysis Model

As discussed above, every dynamical model can follow the phase- space of nucleons only and therefore one need to define the clusters. These methods are referred as "secondary models". In a very simple picture, nucleons were connected to a cluster using space correlation method. This method binds two nucleons in the same fragment if their centroids are less than certain distance [20]. This method is called as Minimum Spanning Tree method [21]. By default this method is valid for dilute systems and therefore cannot address the question of mechanism behind the multi-fragmentation which may happen at relative higher densities. This method is one of the most extensively used methods. Recently, several modified versions of the MST method and some new algorithms were also advanced. Some of these methods are based on the spatial-momentum correlations whereas other needs proper minimization of the energy of the system. We shall discuss these methods in detail in chapter 2.

From the above discussion, it is clear that several primary and secondary models are available to study the reaction dynamics. We shall use the IQMD model coupled with minimum spanning tree method (MST), minimum spanning tree with momentum cut (MSTP) and minimum spanning tree with binding energy check (MSTB). Here, we shall study different asymmetric reactions. The symmetric reactions generate high compression

whereas asymmetric reactions lead to heat or thermal energies. The collision of a heavy target against light projectile gives possibility target multi-fragmentation whereas the collision of a heavy projectile against light target gives possibility of projectile fragmentation mechanism. Moreover, the physics at peripheral collisions is dominated by the spectator whereas the central collision has a fire ball dynamics.

References

[1] Ch. Hartnack, R. K Puri, J. Aichelin, J Konopka, S.A.Bass, H.Stocker, W. Greiner, Eur Phys. J. A 1 **151** 169 (1998).

[2] W.Cassing, V Metag, U Mosel and K.Naiita, Phys. Rep. **188** 363 (1990).

[3] H.Stocker and W.Gernier, Phys. Rep. **137**, 277 (1986)

[4] R.K. Puri, N. Ohtsuka, E.Lehmann, A. Faessler, M.A. Matin, D.T. Khao, G. Batko and S.W. Haung, Nucl. Phys. **A 575**, 733V(1994)

[5] Ch.O.Bacri et al.,Int. Workshop on multiparticle correations and nuclear reactions, Nantea, France, p.338 (1994).

[6] L. Phair et al., Phys. Rev Lett.**75**, 213 (1995) ibid **77**,822 (1996)

[7] L.G. Moretto, D.N.Delis and G.J. Wozniak, Phys.Rev.Lett.**71**, 3935(1993)

[8] J. P. Alard *et al*., Phys. Rev. Lett. **69**, 889 (1992)

[9] C.A.Ogilvie *et al*., Phys. Rev. Lett. **67**,1214(1991)

[10] D. Hahn, H.Stocker, Phys. Rev.C **37**, 1048 (1988)

[11] J. Konopka, Ph.D. Thesis, Univ. Frankfurt, (1995)

[12] G. Peilert, A. Rosenhauer, J. Aichelen, H.Stocker and W. Geiner, Mod. Phys. Lett. A **3**, 459 (1998).

[13] J. Aichelin, Phys. Rep. **202**, 233 (1991).

[14] H. Feldmeir, J. Schnack, Proc. Int. Workshop on Dyn. Features of Nuclei, Spain (1993) World Scientific: H. Feldmeir, J.Schnack, Nucl. Phys. A 583, 347c (1995); H. Feldmeir, K. Bieler, J. Schnack, Nucl. Phys. A **586**, 493 (1995).

[15] E. Lehmann, R. K. Puri, A. Faessler, G. Batko and S.W. Huang, Phys. Rev. C **51**, 2113(1995).

[16] A. Bohnet, N. Ohtsuka, J. Aichelin, R. Linden and A. Faessler, Nucl. Phys. A **494**,349(1989).

[17] M. Trefz, A. Faessler and W. H. Dickhoff, Nucl. Phys. A **443**, 499(1985).

[18] J. Cugnon and C. Hartnack and J. Aichelin, Phys. Rev. C **54**(1993).

[19] Ch. Hartnack,Rajeev K. Puri, J.Aichelin et.al., Phys. J.A 1151**,169** (1998)

[20] R.K. Puri and S.Kumar Phys. Rev **C 57** 2744 (1998)

[21] S.Kumar and R.K. Puri Phys. Rev **C 58**, 2858 (1998)

Chapter 2

Methodology

2.1 Introduction

The dynamics at intermediate energy, however, requires the equal weight age to nucleon-nucleon binary collisions and mean field. This demand gives correct information about the real and imaginary parts of the potential. In addition, one also has to deal with the initial non-equilibrated situations that change during the course of the reaction. The dynamical transport models employed at intermediate energies are supposed to include the essential collision physics. In the following, we will discuss about Quantum Molecular Dynamics (QMD), Isospin Quantum Molecular Dynamics Model (IQMD) [1-3].

.

2.1.1 Molecular Dynamics and Need of Quantum Dynamics Approach

The classical molecular dynamics (MD) [1-3] approach is capable of treating both compression and fragment formation. The molecular dynamics predicts the collective flow in a qualitative agreement with the data. It incorporates the complete classical N-body dynamics which is necessary to describe the formation of fragments. Naturally, the simple classical molecular dynamics needs refinement which should also involves quantum features. In nuclear physics, the key problem in MD methods lies in the treatment of the Pauli principle. Nucleons are fermions and it is difficult to speak of nuclei without the Pauli principle. This question is simply overlooked in strictly classical calculations. MD methods with Pauli principle address this question but with disputable success. So we need a quantum dynamics approach to speak of nuclei with Pauli principle which are explained by QMD and IQMD Models.

2.2 Quantum Molecular Dynamics

The quantum molecular dynamics model [4-5] is based on the molecular dynamics picture where nucleons interact via two- and three-body interactions. The explicit two- and three-body interactions lead to the preservation of the fluctuations and correlations which are important for *N*-body phenomena like multifragmentation.

The QMD model contains the following ingredients: short-range interaction (hard-core repulsion), stochastic scattering with energy cross sections, particle production, Fermi motion of the nucleons as well as the quantum effect of the Pauli blocking.

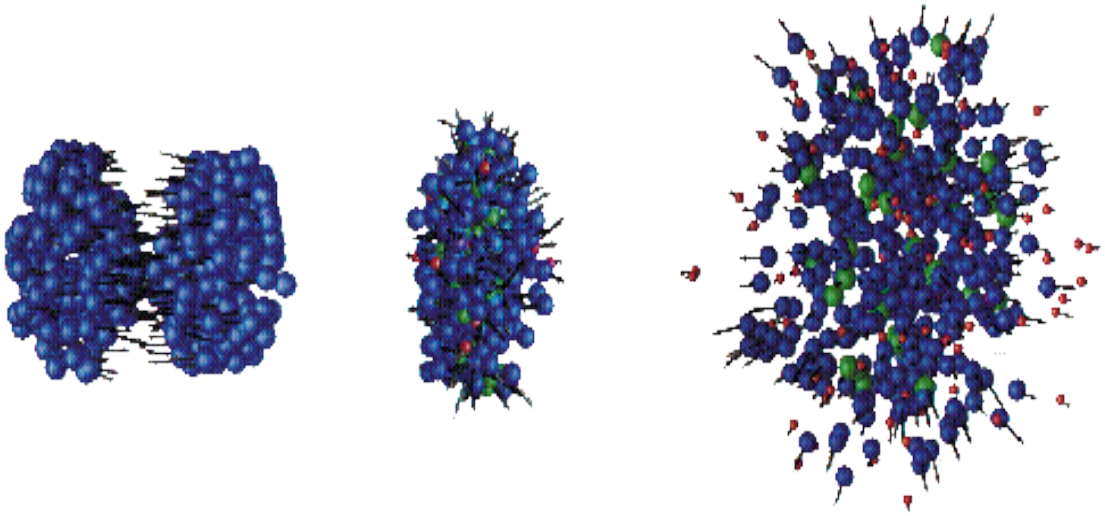

Fig 2.1 shows the initialization, propagation, collision in QMD Model.

The simulation in QMD model needs three steps:

1. **Initialization**: one has to generate the nuclei.
2. **Propagation**: then, these nucleons propagate under the influence of surrounding mean field.
3. **Collision**: finally, the nucleons are bound to collide, if they come close to each other.

2.2.1 Initialization

In QMD, the successfully initialized nuclei are boosted towards each other with proper center-of-mass velocity using relativistic kinematics [4]. Here each nucleon is represented by a Gaussian wave packet with a width √L centered around the mean position $\vec{r}_i(t)$ and the mean momentum $\vec{p}_i(t)$:

$$\Phi_i(\vec{r},\vec{p},t) = \frac{1}{(2\pi L)^{3}/_{4}}\, e^{\{-\frac{[\vec{r}-\vec{r}i(t)]^2}{4L}\}} e^{[i\vec{p}(t).\frac{\vec{r}}{h}]} \qquad (2.1)$$

The parameter L, which is related to the extension of the wave packet in phase space is fixed.The total N-body function is assumed to be a direct product of the coherent states. The Wiegner distribution of a system with A_T+A_P nucleon is given by:

$$f_i(\vec{r},\vec{p},t) = \frac{1}{(\pi h)^3}\, e^{\{-\frac{[\vec{r}-\vec{r}i(t)]^2}{2L}\}} e^{\{-\frac{[\vec{p}-\vec{p}i(t)]^2\ 2L}{h^2}} \qquad (2.2)$$

With L=1.08 fm^2. In other words, the r.m.s radius of a nucleon is about 1.8 fm and hence is almost twice as large as that obtained from electron scattering. A smaller value of L is excluded because the nuclei would become unstable after initialization. Thus, this value of L presents the limit for a semi classical theory [4]. The value of L determines the interaction range of the particle and influences the density distribution of a finite system.

2.2.2 Propagation

The nucleons are propagated under the total interaction calculated by the Hamiltonian equations of motion

$$\dot{p}_i = -\frac{\delta\langle H\rangle}{\delta r_i}, \qquad \dot{r}_i = \frac{\delta\langle H\rangle}{\delta p_i}$$

A total Hamiltonian function with a kinetic energy T and a potential energy V results:

$$H = T + V = \sum_i \frac{p_i^2}{2m_i} + \sum_i \sum_{j>i} \int f_i(\vec{r}, \vec{p}, t) V^{ij} f_j(\vec{r'}, \vec{p'}, t)\, d\vec{r}\, d\vec{r'}\, d\vec{p}\, d\vec{p'} \quad (2.3)$$

The potential in equation (2.3) is the sum of the following specific elementary potentials,

$$V = V_{loc} + V_{Yuk} + V_{Coul} + V_{mdi} \quad (2.4)$$

with the local hard-core repulsion,

$$V_{loc} = \sum_i \sum_{j>i} t_1\, \delta(\vec{r_i} - \vec{r_j}) + \sum_i \sum_{j>i} \sum_{k>j} t_2\, \delta(\vec{r_i} - \vec{r_j})\, \delta(\vec{r_i} - \vec{r_k}), \quad (2.5)$$

The Yukawa long-range term,

$$V_{Yuk} = \sum_i \sum_{j>i} t_3 \frac{e^{\frac{|\vec{r_i} - \vec{r_j}|}{a}}}{\frac{|\vec{r_i} - \vec{r_j}|}{a}}, \quad (2.6)$$

The Coulomb term with only a mean value for the nucleon charge because QMD does not know the isospin of the particles,

$$V_{Coul} = \frac{Z}{A} \sum_i \sum_{j>i} \frac{e^2}{|\vec{r_i} - \vec{r_j}|} \quad (2.7)$$

and the momentum dependent interaction

$$V_{mdi} = \sum_i \sum_{j>i} t_4 \ln(1 + t_5 (\overrightarrow{p_i} - \overrightarrow{p_j})^2) \delta(\vec{r_i} - \vec{r_j}) \quad (2.8)$$

Parameters used in equations (2.3) to (2.8) can be found in table 2.1.

(I)QMD parameters	
t_3	15 MeV
t_4	1.57 MeV
t_5	$5x10^{-4}$ MeV^{-2}
t_6	25 MeV
a	1.5 fm

Table 2.1: QMD parameters used in equations (2.3) to (2.8).

Another important ingredient in the model is the nucleon- nucleon collision which is characterized by the nucleon- nucleon cross section. We shall use here an energy dependent nucleon- nucleon cross- section [5].

2.2.3 The Nucleon- Nucleon Collision

During the propagation, two nucleons can collide, if they come close to each other. The effect of N-body collision is found to be rather small; therefore we neglect N- body collisions. The collisions in QMD are treated as in the same way as in BUU model. Two particles undergo scattering if they are closer than a distance $\sqrt{\frac{\sigma_{tot(s)}}{\pi}}$ [6]. This scattering is further subject to the fulfillment of Pauli- principle. If the final state of scattered nucleons violates the principle, the collision is neglected. Here ($\sqrt{\sigma_{tot}}$) represents the total NN cross section and √s is the centre-of-mass energy.

The impact of in- medium cross-sections is drastic at low- energies. With increase in the incident energy, these effects start washing away and thus the medium cross section

approaches the free nucleon-nucleon cross section. On the other hand, with an increase in the bombarding energy, the velocity of particles becomes comparable to the velocity of light, therefore the relativistic effects becomes very important [7].

2.2.4 Pauli Blocking

Whenever a collision occurs, the phase space around the scattering partners is checked. For simplicity, we assume that each nucleon occupies a sphere in coordinate and momentum space [8]. This trick yields the same Pauli blocking ratio as an exact calculation of the overlap of the Gaussians will yield. We calculate the fractions P_1 and P_2 of final phase space for each of the two scattering patterns is already occupied by other nucleons. The collisions are blocked with a probability which is given by:

$$P_{Block} = 1-[1-\min(P_1,1)][1-\min(P_2,1)] \quad (2.9)$$

And is allowed with probability $1-P_{block}$. For a nucleus in its ground state, we obtain an averaged blocking probability $< P_{block} >$ of 0.96. For absolute blocking, this factor should be one. From above description, it is clear that the Pauli factor will be zero or one depending whether the final phase- space is occupied or not. This sharp occupancy is valid for the cold nuclear matter only.

2.3 Isospin Quantum Molecular Dynamics (IQMD)

Quantum molecular dynamics (QMD) model contains two dynamical ingredients, the density dependent mean field and the in-medium nucleon nucleon cross-section. In order to describe the isospin dependence appropriately, the QMD model should be modified properly. Considering the isospin effects in mean field, two-body collision and Pauli blocking, important modifications in QMD have been made to obtain an isospin dependent quantum molecular dynamics (IQMD). Therefore, for an isospin-dependent reaction

dynamics model, it is essential that all three components should reasonably include isospin degrees of freedom.

The Isospin-QMD (IQMD) treats the different charge states of nucleons, deltas and pions explicitly, as inherited from the VUU model. IQMD has been used for the analysis of collective flow effects of nucleons and pions. As it has been developed from the VUU-model, its coding is therefore, independent of the original QMD. The isospin degrees of freedom enter into the cross sections (here cross sections of VUU similar to the parametrizations of VerWest and Arndt have been taken, see also) as well as in the Coulomb interactions. The elastic and inelastic cross sections for proton-proton and proton-neutron collisions used in IQMD are shown in Fig. 2.2. The cross section for neutron-neutron collisions is assumed to be equal to the proton-proton cross sections [9].

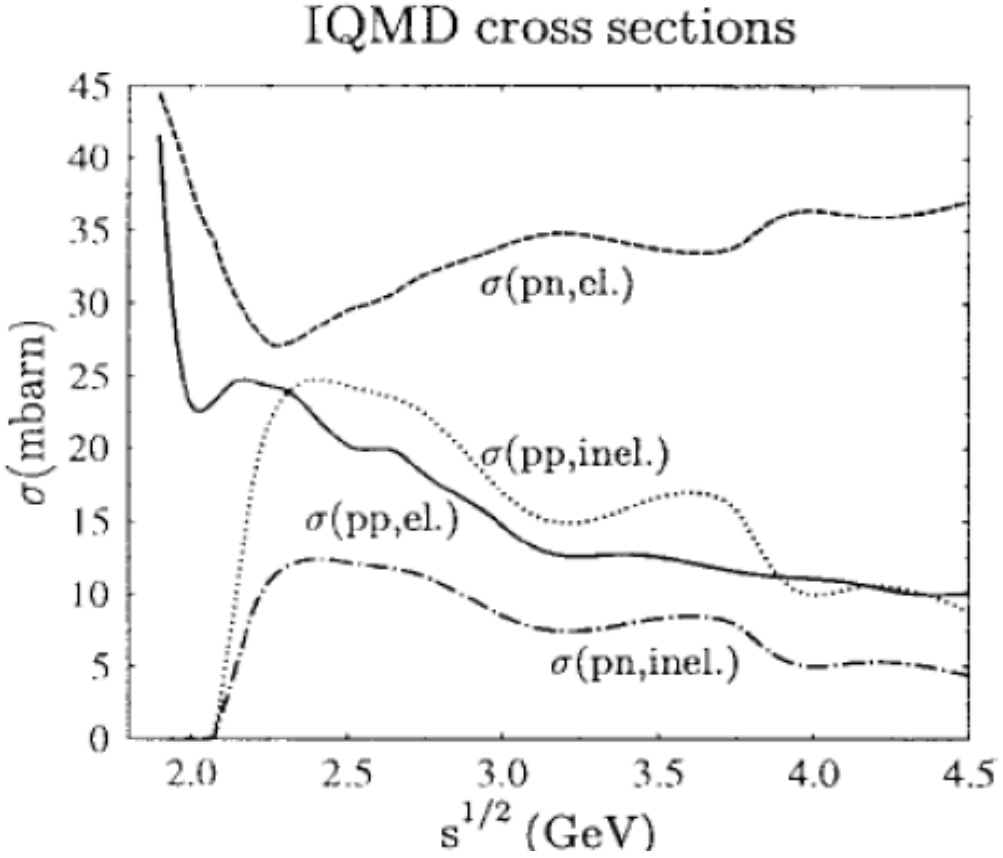

Fig 2.2. The elastic and inelastic cross sections for proton-proton (pp) and proton neutron (pn) used in IQMD.

In addition, it is also important that, in initialization of projectile and target nuclei, the samples of neutrons and protons in phase space should be treated separately since there exist a large difference between neutron and proton density distributions for nuclei far from the β stability line. Particularly, for neutron rich nucleus one should sample a stable initialized nucleus with neutron-skin structure and therefore one can directly explore the nuclear structure effects through a microscopic transport model. The IQMD model has been improved based on the above ideas. The following describes briefly IQMD model from four aspects, i.e., initialization, potentials used in IQMD, collisions and Pauli blocking,

2.3.1 Initialization in IQMD

In IQMD, the centroids of the Gaussians in a nucleus are randomly distributed in a phase space sphere ($r \leq R$ and $p \leq p_F$) with $R = 1.12\ A^{1/3}$ fm corresponding to a ground state density of $\rho_0 = 0.17\text{fm}^{-3}$. The Fermi momentum p_F depends on the ground state density. For $\rho_0 = 0.17\text{fm}^{-3}$ it has a value of about $p_F \approx 268$ MeV/c. In IQMD the momenta are uniformly distributed within a momentum sphere $p \leq p_{Fermi} \approx 268$ MeV/c without further local constraints. Therefore it may happen that nucleons close to the surface, where the local potential energy is low, are unbound initially. This possibility is not given in BQMD or HQMD. It gives, however, a reduced binding energy per nucleon as compared to the Weizsacker mass formula. Hence the initialized nuclei are less stable against spurious particle evaporation. Finally it should be noted that IQMD performs a Lorentz contraction of the nucleus coordinate distribution which is not present in QMD and which becomes important for higher energies E/nucleon > 1 GeV.

In IQMD particles are represented by the one particle Wigner density.

$$f_i(\vec{r},\vec{p},t) = \frac{1}{(\pi h)^3}\, e^{\{-\frac{[\vec{r}-\vec{r}i(t)]^2}{2L}\}} e^{\{-\frac{[\vec{p}-\vec{p}i(t)]^2\, 2L}{h^2}} \qquad (2.10)$$

with L=1.08 fm^2. In other words, the r.m.s radius of a nucleon is about 1.8 fm and hence is almost twice as large as that obtained from electron scattering. A smaller value of L is excluded because the nuclei would become unstable after initialization. Thus, this value of

L presents the limit for a semi classical theory [9]. The value of *L* determines the interaction range of the particle and influences the density distribution of a finite system. Here, the system size dependence of L value is taken into account which is 4L=4.33 fm^2 for lighter system while 4L=8.66 fm^2 is for heavier system.

In a semi classical theory, this parameter is chosen by the stability of nuclei generated. Ideally, a time dependent width of the Gaussian should be used. The Gaussian width for a particular nucleon is chosen in a way so that maximum stability of the nucleonic density profile can be achieved. A detailed study of the effect of different interaction ranges on different observable is carried out in [8,9]. An extended wave packet will connect a large number of nucleons in a fragment and as a result, it will generate heavier fragments compared to the one obtained with a smaller width. The effect of doubling the width is, by taking fragmentation as the latter reduces the multiplicity of intermediate mass fragments to a large extent. One should, however, keep in the mind that this effect depends on the physical situation and condition.

2.3.2 Potentials used in IQMD

The total one particle Wigner density is the sum of all nucleons. The expectation value of the total Hamiltonian is

$$\langle H \rangle = \langle T \rangle + \langle V \rangle$$

$$= \sum_i \frac{p_i^2}{2m_i} + \sum_i \sum_{j>i} \int f_i(\vec{r}, \vec{p}, t) V^{ij} f_j(\vec{r}', \vec{p}', t) d\vec{r}\, d\vec{r}' d\vec{p}\, d\vec{p}' \qquad (2.11)$$

The baryon-potential consists of the real part of the G-Matrix which is supplemented by the Coulomb interaction between the charged particles. The former can be further subdivided in a part containing the contact Skyrme-type interaction only, a contribution due to a finite range Yukawa-potential, and a momentum dependent part.

$$V^{ij} = G^{ij} + V_{Coul}^{ij} = V_{Skyrme}^{ij} + V_{Yuk}^{ij} + V_{mdi}^{ij} + V_{Coul}^{ij} + V_{sym}^{ij}$$

$$= t_1\delta(\vec{x}_i - \vec{x}_j) + t_2\delta(\vec{x}_i - \vec{x}_j)\rho^{\gamma-1}(\vec{x}_i) + t_3\frac{exp\{-|\vec{x}_i - \vec{x}_j|/\mu\}}{|\vec{x}_i - \vec{x}_j|/\mu}$$

$$+ t_4 ln^2\left(1 + t_5(\vec{p}_i - \vec{p}_j)^2\right)\delta(\vec{x}_i - \vec{x}_j) + \frac{Z_i Z_j e^2}{|\vec{x}_i - \vec{x}_j|} + t_6\frac{1}{\varrho_0}T_3^i T_3^j \delta(\vec{r}_i - \vec{r}_j)$$

(2.12)

The parameters t_1...t_5 are uniquely related to the corresponding values of α, β, γ, δ and ϱ which serve as input. It is a combination of Skyrme type and momentum dependent potential with a low compressibility.

In the description of the Coulomb interaction V_{ij}^{coul}, Z_i, Z_j are the charges of the baryons i and j. The momentum dependence of V_{ij}^{mdi} the N–N interaction, which may optionally be used in QMD, is fitted to experimental data [10,11] on the real part of the nucleon optical potential [12,13], which yields

$$U_{mdi} = \delta . ln^2(\varepsilon.(\Delta\vec{p})^2 + 1).\left(\frac{\rho_{int}}{\rho_0}\right)$$

(2.13)

The IQMD-model offers rather stable density distributions and good energy conservation, however for the price of nucleon evaporation and improper binding energies ($E_{bind} \approx 4-5$ MeV/nucleon for heavy nuclei instead of 8 MeV/nucleon). In addition to the use of the explicit charge states of all baryons and mesons a symmetry potential between protons and neutrons corresponding to the Bethe-Weizsacker mass formula has been included

$$V_{sym}^{ij} = t_6\frac{1}{\varrho_0}T_3^i T_3^j \delta(\vec{r}_i - \vec{r}_j) \qquad t_6 = 100MeV$$

(2.14)

Where T_3^i and T_3^j denote the isospin T_3 of the particles i and j, i.e. 1/2 for protons and -1/2 for neutrons. The potential part of the equation of state resulting from the convolution of the distribution functions f_i and f_j with the interactions V_{sym}^{ij}+ V_{mdi}^{ij}(local interactions including momentum dependence) reads:

$$U = \alpha.\left(\frac{\rho_{int}}{\rho_0}\right) + \beta.\left(\frac{\rho_{int}}{\rho_0}\right)^{\gamma} + \delta.ln^2(\varepsilon.(\Delta\vec{p})^2 + 1).\left(\frac{\rho_{int}}{\rho_0}\right) \quad (2.15)$$

2.3.4 Collision

Two particles collide if their minimum distance d, i.e. the minimum relative distance of the centroids of the Gaussians during their motion, in their CM frame fulfills the requirement:

$$d \leq d_0 = \sqrt{\frac{\sigma_{tot}}{\pi}}, \quad \sigma_{tot} = \sigma\left(\sqrt{s}, type\right) \quad (2.16)$$

where the cross-section is assumed to be the free cross section of the regarded collision type (N − N, N − Δ, . . .). The total cross-section is the sum of the elastic cross -section and all inelastic cross-sections.

$$\sigma_{tot} = \sigma_{el} + \sigma_{inel} = \sigma_{el} + \sum_{channels} \sigma_i \quad (2.17)$$

For instance for a pp collision we may have

$$\sigma_{tot} = \sigma_{el} + \sigma(pp \rightarrow p\Delta^+) + \sigma(pp \rightarrow n\Delta^{++}) \quad (2.18)$$

The cross-sections for the different channels are given by experiment or by spin/isospin coeffiicents.

For the pp case for example we have

$$\sigma(pp \rightarrow n\Delta^{++}) = 3\sigma(pp \rightarrow p\Delta^{+}) = \frac{3}{4}\sigma_{inelastic} \qquad (2.19)$$

Inaccessible reactions like ΔN → NN are calculated from their reverse reactions (here NN → ΔN) using detailed balance method. The possibility of reaching a channel in a collision is given by its contribution to the total cross-section

$$P_{channel} = \frac{\sigma_{channel}}{\sigma_{tot}} \qquad e.g. \quad P_{pp\rightarrow p\Delta^{+}} = \frac{1}{4}\frac{\sigma_{tot}-\sigma_{el}}{\sigma_{tot}} \qquad (2.20)$$

2.3.5 Pauli Blocking

The method of considering the Pauli blocking effect is whenever a collision has occurred, in the phase space we assume that each nucleon occupies a six dimensional sphere with a volume of $h^3/2$ (considering the spin degree of freedom), and then calculate the phase volume V, of the scattered nucleons being occupied by the rest nucleons with the same isospin as that of the scattered ones. We then compare $2V/h^3$ with a random number and decide whether the collision is blocked or not. Therefore, the Pauli blocking is isospin dependent, namely, the Pauli blocking of neutrons and protons is treated separately. In addition, Pauli blocking (of the final state) of nucleons is taken into account by checking the phase space densities in the final states [12].

The final phase space fractions P_1 and P_2, which are already occupied by other nucleons are determined for each of the scattering nucleons. The collision is then blocked with probability.

$$P_{block} = 1 - (1 - P_1)(1 - P_2). \qquad (2.21)$$

2.4 Cluster analysis

We shall use the following algorithms for clusterizing in which the phase generated by a IQMD model.

2.4.1 Spatial correlation algorithm (Minimum spanning tree method)

In a spatial correlation method, two nucleons are allowed to share the same fragment if their centroids are closer than a distance d_{min} i.e. 4 fm [13].

$$r_i - r_j \leq d_{min} \approx 4fm \qquad (2.22)$$

where r_i and r_j are the spatial positions of both nucleons. The minimum distance d_{min} has been used as a free parameter which varies between 2-4 fm. Its influence on multifragmentation (at 200-300 fm/c) is to be small. This approach (being a spatial distance approach) cannot detect fragments which are almost overlapping and therefore, will give a single big fragment during the early stage of reaction where density is quite high and the interaction among the nucleons are still active. By definition, this method cannot address the time scale of fragmentation. This single large fragment at the time of high density gets split into several light and medium mass fragments after the lapse of several 100 fm/c. This is called minimum spanning tree (MST) method. It is worth mentioning that this method can only be used to analyze asymptotic configurations in which the fragmenting system can be viewed as a very dilute mixture of free particles and almost equilibrated fragments.

2.4.2 Spatial and momentum correlation algorithms

a. Momentum cut(MSTM)

An improvement over the MST algorithm is to put additional cut in momentum space. It will help to get rid of fragments that although close in spatial space are far in momentum space. The MSTM method also takes care of the relative momentum of nucleons. In

addition to equation (2.22) we also check the relative momenta of the nucleus. Therefore, we say two nucleons must obey equation (2.23) [14].

$$p_i - p_j \leq p_{fermi} \tag{2.23}$$

where p_{fermi} is the average Fermi momentum of the nucleons bound in a nucleus at its ground state which is about 268 MeV/c in IQMD. This definition, discards all those nucleons which are too far in their momentum space. We term this extension the minimum spanning tree method with a momentum cut (MSTM method). This additional condition avoids the creation of unbound or weakly bound fragments in central symmetric collisions at higher incident energies.

b).<u>Binding energy check</u>

This is a modified version of the normal MST method where the pre-clusters obtained with MST method are subjected to binding energy condition [15].

$$\zeta_f = \frac{1}{N^f} \sum_{i=1}^{N^f} \left[\sqrt{(\overrightarrow{p_i} - \overrightarrow{p_{cm}})^{\,2} + m_i^2} - m_i + \frac{1}{2} \sum_{1 \neq j}^{N^f} V_{IJ} \right] < E_{BIND} \tag{2.24}$$

Here we take E_{bind} = -4.0. MeV if $N^f \geq 3$ and $E_{bind} = 0$. In this equation, N^f represents the number of nucleons bound in a fragment and p_{cm} is the centre of mass momentum in a fragment. The requirement of a minimum binding energy excludes the loosely bound fragments which will decay at a later stage. The precise value of the E_{bind} changes the fragment multiplicity slightly at intermediate stage but no influence on the qualitative behaviour. If any pre-cluster fails to meet the binding energy condition equation (2.24). This pre-cluster is treated as unbound and all the nucleons of such a pre-cluster are treated as free nucleons. Naturally, such a binding energy condition is applied to fragments with mass ≥ 3. This modified method is dubbed as minimum spanning tree with binding check (MSTB)method[16].All of unbound fragments (with binding energy/nucleon less than 4 MeV) will automatically be discard[14].This method was quite useful for central collisions at higher incident energies where a lot of excited fragments are created

References

[1] Suneel kumar, Sanjeev kumar and Rajiv. K. Puri. Phys. Rev. **C 81**, 014611 (2010).

[2] P.Danielewicz, R.Lacey and W. G. Lynch, science **298**, 1592 (2002); H. Stocker and W. Greneir, Phys. Rep **137**,273 (1986); W. Reisdrof and H.G. Ritter, Annu. Rev. Nucl. Sci. **47**, 663 (1997); C. Hartnack and J. Aichelin Phys. Rev. C **49**, 2801 (1994); S. Kumar, S.Kumar and R. K. Puri ibid **78**, 064602 (2008); A. R. Raduta and F.Gulminelli, ibid 75, 024605 (2007).

[3] Suneel Kumar, Ph.D. Thesis, P.U. Chandigarh (1999).

[4] J. Aichelin, Phys. Rep. **202**, 233 (1991).

[5] G. Peilert, A. Rosenhauer, J. Aichelen, H.Stocker and W. Geiner, Mod. Phys. Lett. A **3,** 459 (1989).

[6] G. Batko, J.Randrup and T.Vetter, Nucl. Phys. **A 536,** 786 (1992); G.Batko, J. Randrup and T. Vetter, Nuclei. Phys. **A 546**, 761 (1992)

[7] R.K. Puri, E. Lehmann, A. Faeseler and S.W. Haung, J. Phys. **G 21, 583** (1995)

[8] R.K. Puri, N. Ohtauska, E. Lehmann, A. Faessler, M.A. Matin, D.T. Khao, G.Batko and S.W. Haung, Nucl. Phys. **A 546**, 761 (1992)

[9] Ch. Hatrtnack, Rajeev K. Puri, J. Aichelin..Eur. Phys. J.A. 1 151-169(1998).

[10] Chen Liewen, Zhang Fengshou, and Jin Genming Phys. Rev. **C 58,** 2283 (1998).

[11] Suneel Kumar, Sanjeev Kumar and Rajeev. K. Puri. Phys. Rev. **C 81**, 014601 (2010).

[12] L. G. Arnold et al., Phys. Rev. C **25**, 936 (1982).

[13] S.Kumar and R.K. Puri Phys. Rev **C 58**, 320 (1998)

[14] R.K. Puri and S.Kumar Phys. Rev.**C 58**,2858 (1998).

Chapter 3

The Clusterization Algorithms in Multifragmentation

3.1 Introduction

In past years, a lot of efforts have been made experimentally and theoretically to understand the multifragmentation and its associated properties. It is well known that the colliding nuclei (at intermediate energies) shatter into several small, medium size pieces as well as lot of nucleons are also emitted which is dubbed as multifragmentation. There are several features of multifragmentation which were observed as a function of bombarding energies and impact parameter. This includes the rise and fall in fragment production with change in the impact parameter. As we discussed in chapter 1, on the basis of theoretical scenario, one has the dynamical model where the reaction dynamics starts simulation from well defined nuclei to the end of the reaction where it practically cold and scattered nuclear matter in the form of nucleons i.e. light or heavy mass fragments [1-2]. Therefore, no dynamical model simulates the fragments, rather one has the phase space of nucleons and one constructs the fragments at the end of simulations. Therefore, we look for secondary models i.e. clusterization algorithms MST, MSTP and MSTB [10-11] which are explained in chapter 2

Experiments have demonstrated that appropriately excited nuclear systems will undergo a multifragment disintegration leading to a final state composed of a mixture of fragments of charge $3 \leq Z \leq 30$ and light particles with $Z \leq 2$. Fragments are produced with large multiplicities in central heavy ion collisions at incident energies of $E_{beam}/A \leq 100$ MeV, at larger impact parameter in heavy ion collisions at $E_{beam}/A \geq 200$ MeV, and in central light ion induced reactions at $E_{beam}/A \geq 5$ GeV.

Fig 3.1 schematically describes the collision stages in reactions between a 5 GeV/nucleon hydrogen ion and a gold nucleus. In the initial stage, heat is deposited into the nucleus and then it is accompanied by the knockout of several fast particles. The hot

nucleus is then thermalized and expands, eventually undergoing a "soft explosion, or multifragmentation

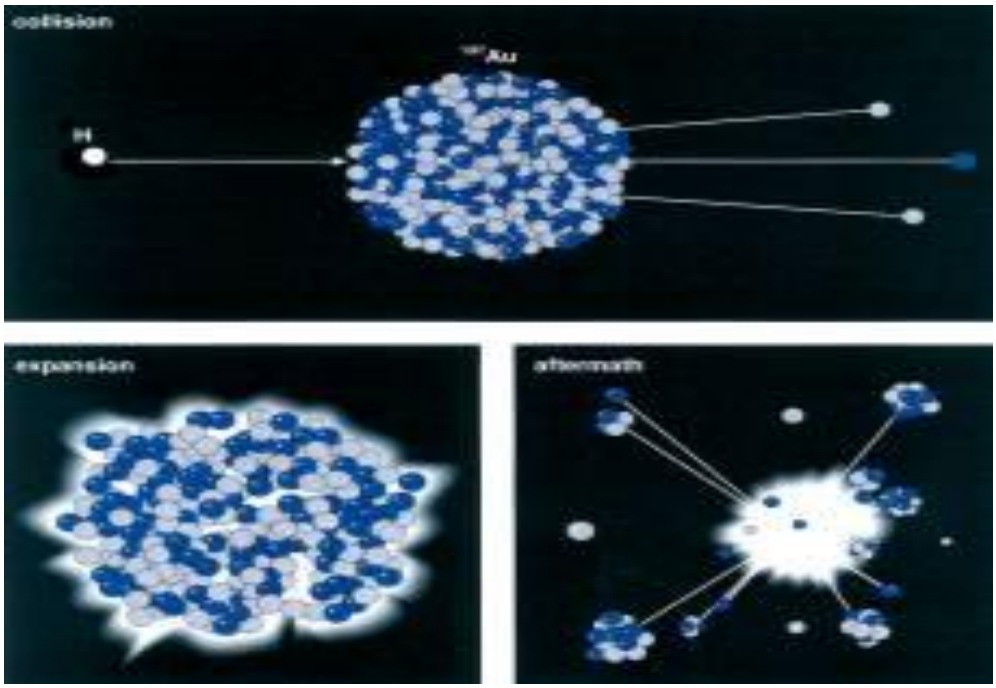

Fig 3.1. Schematic diagram of the collision stages in reactions between a 5 GeV /nucleon hydrogen ion and a gold nucleus.

3.2 Results and discussion

For the present analysis, we simulate two different reactions $^{129}Xe_{54}+^{197}Au_{79}$ at E= 50 MeV/nucleon and $^{36}Ar_{18}+^{197}Au_{79}$ at E =50, 80,110 MeV/nucleon respectively. These reactions are simulated at different impact parameters using hard and soft equation of state at different incident energies with IQMD model. For each reaction 1000 events have been generated using Monte-Carlo technique. The stored phase space is then analyzed by using MST, MSTP and MSTB algorithms.

3.3 Time evolution of density and N-N collisions

The final form of nuclear matter is closely related to the density of collision. We define the average nuclear density as

$$\langle \rho(\mathrm{r_i}) \rangle = \langle \sum_{j=0}^{n} \frac{1}{(2\pi L)^{3/2}} e^{-(\vec{r_i}-\vec{r_j})^2/2L} \rangle$$

The above density definition shows the number of nucleons in the vicinity of each nucleon. Fig.3.2(a) and 3.2(b) shows the scaled density (ρ/ρ_0) with respect to time and the variation of allowed collisions for the different reactions $^{129}Xe_{54}$ +$^{197}Au_{79}$ at E=50MeV/nucleon and $^{36}Ar_{18}$+ $^{197}Au_{79}$ at E =50, 80, 110 MeV/nucleon. Here we consider the case of central collisions only. We noticed that density is closely related to the rate of collisions.

We observed that the rate of collisions for system$^{36}Ar_{18}$+$^{197}Au_{79}$ at E=50 MeV/nucleon is small (shown in fig 3.2(b)) as compared to the other targets. This is because of the small size of projectile as compared to the target, so very less overlapping will takes place. In other words, one can say this reaction is highly asymmetric and the overlapping region is small, leading to the less destruction of the system. In other words, the spectator matter is not too much affected. Due to this very less charge is observed in the trajectory and hence minimum change in the time evolution of density will be observed for the highly asymmetric system. On the other hand, with increase in symmetry of the system, overlapping zone will increase; destruction of the system will increase. Due to increase in the number of collision, system will take large time to become cold and stable. This will result in decrease in the density at the saturation time with increase in the symmetry of the system. One may be noted that opposite trend is observed for the density at the time of maximum compression.

In case of $^{129}Xe_{54}$ +$^{197}Au_{79}$ E=50 MeV/nucleon, maximum number of collisions are observed because both target and projectile are of comparable size hence lesser is the density, one can see from the figure.

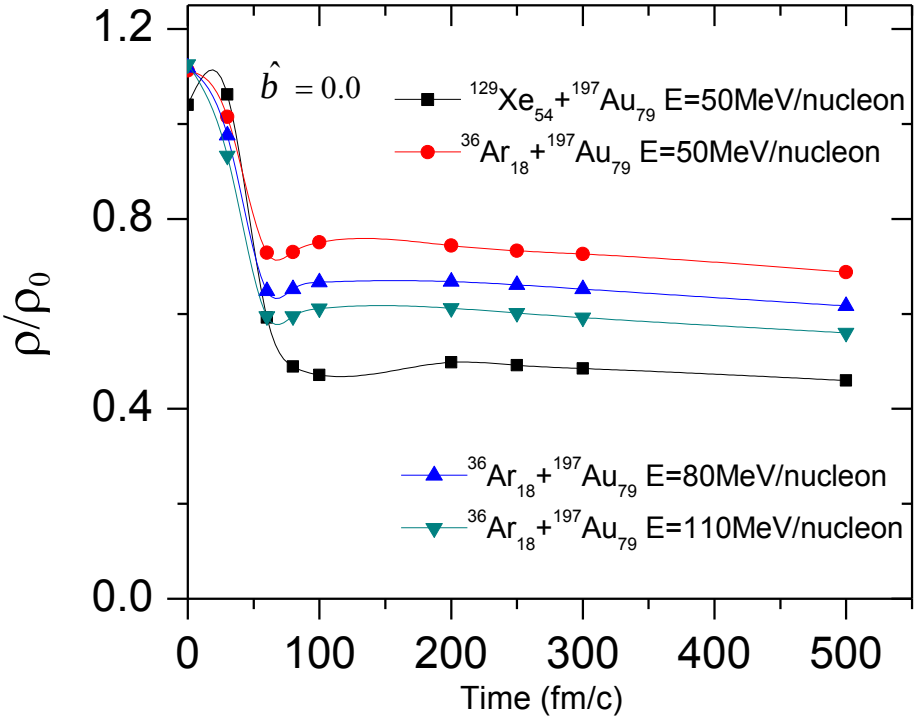

Fig: 3.2(a). Time evolution of density with hard EOS

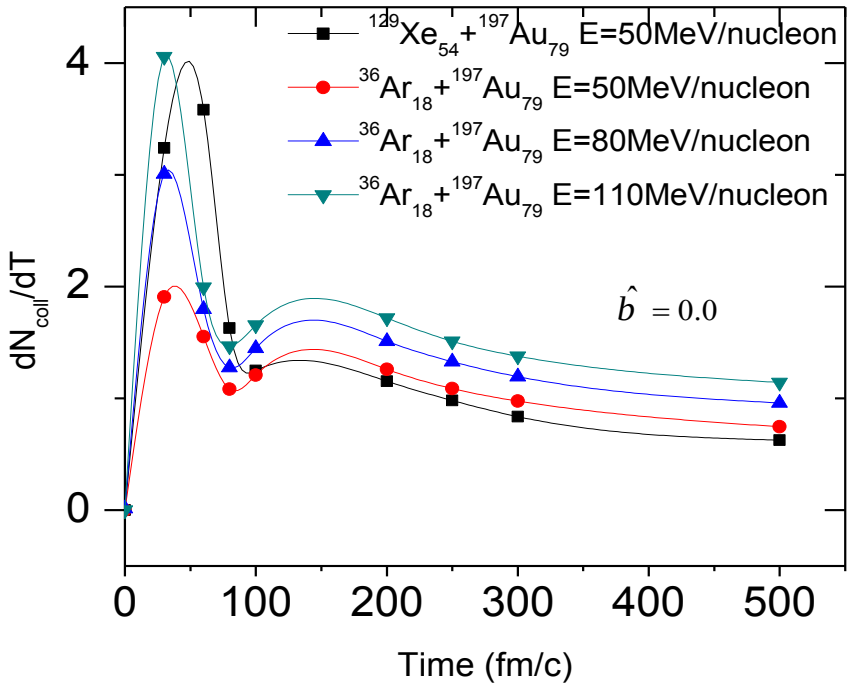

Fig: 3.2(b). Time evolution of allowed collision with hard EOS

3.4 Time evolution as a function of multiplicity

Fig 3.3 displays the time evolution of different fragments with 2≤A≤4 and 5≤A≤9 and 5≤A≤54 for $^{129}Xe_{54}+^{197}Au_{79}$ at E=50MeV/nucleon with three different algorithms i.e. MST, MSTP MSTB at $\hat{b}$ =0.4 fm using hard equation of state. In case of free nucleons using MST indicates 197 nucleons at t=0 which increase to 326 nucleons at 30 fm/c. A cluster consisting of 326 nucleons at 30 fm/c signifies that nuclear matter is compressed and there is high density phase. As two nuclei (i.e. target and projectile) have large relative momenta and compound nucleus is not stable and it decays by emitting light and intermediate mass fragments.

In other words, we have an artificial phenomenon in MST and MST shows all nucleons as unbound but MSTB and MSTP identifies the free nucleons as early as possible. Also MSTB and MSTP is the extension of MST method. In MSTB, we first get the pre-clusters using MST and then check the binding energy of each fragment. In other words, if the fragments in MST are properly bound, then the MST, MSTP and MSTB give same results. But if MST gives unbound fragments then the fragment distribution using MSTB will differ from that of MST. MSTP and MSTB discard those fragments which are weakly bound or unbound. The time evolution of different fragments with masses 2≤A≤4 and 5≤A≤54 gives several interesting results. In the two cases, a check in the form of binding energy and momentum cut helps to identify the fragments quite early. The normal MST takes quite a long time to identify the stable fragments which are residual of excited fragments [4-5]. The lighter and intermediate mass fragments plays as a result of interplay between the repulsive nucleon-nucleon scattering and attractive mean field.

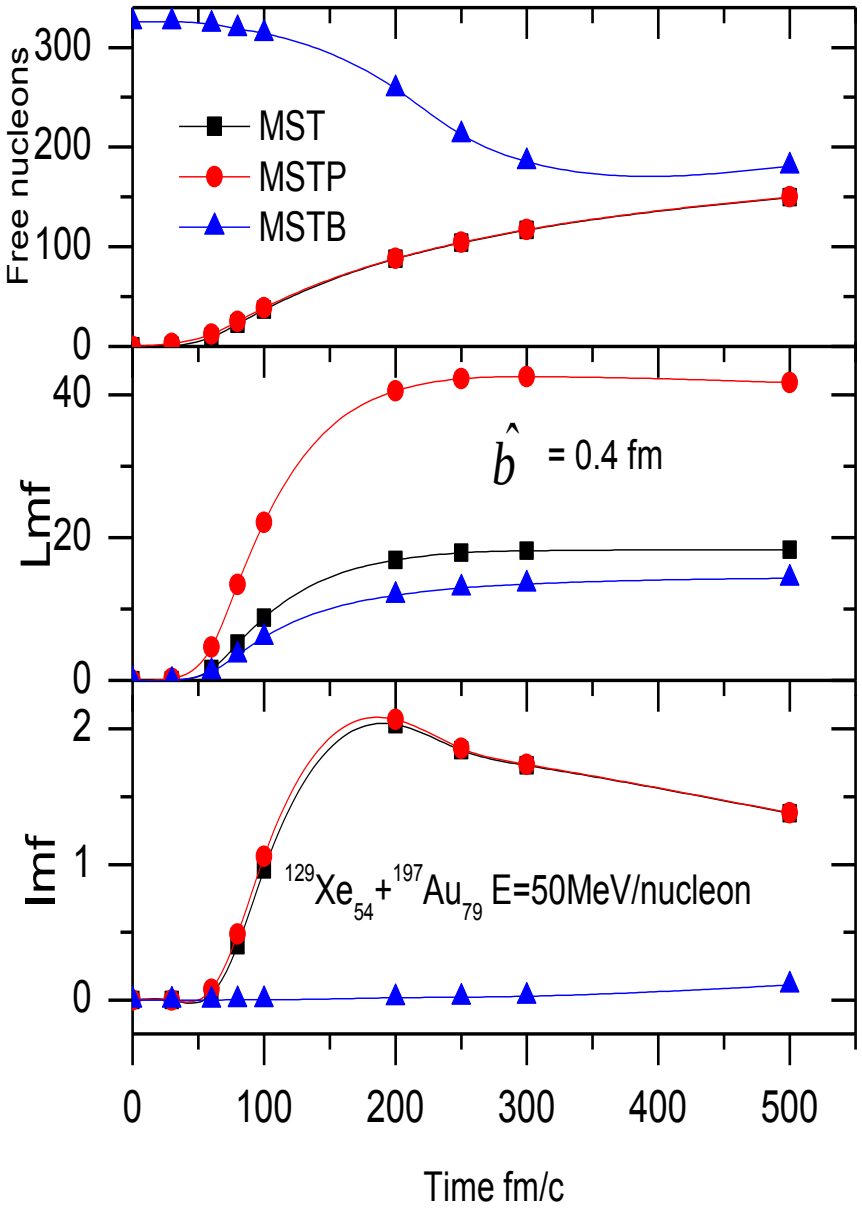

Fig 3.3: The time evolution of different fragments with MST,MSTP and MSTB method.

3.5 Rapidity distribution

Rapidity is one of the important parameter in heavy ion collisions. Rapidity distribution is assumed to give information about the degree of thermalization and stopping achieved in the reaction**.** In fig 3.4, we display the rapidity distribution for jth nucleon which is defined as

$$y_j^f = \frac{1}{2}\ln\frac{E_j^f + p_j^f\ c}{E_j^f - p_j^f\ c}$$

Here E_j^f and p_j^f are the total energy per nucleon and longitudinal momentum per nucleon of jth nucleons [6]. The displayed result is for ^{129}Xe+^{197}Au at E=50MeV/nucleon for free nucleon, LMF, IMF fragments at impact parameter $\hat{b}$=0.4 and $\hat{b}$=0.0 using hard equation of state.

Rapidity distribution indicates the degree of thermalization reached in a system. Narrower is the Gaussian, more is thermalized in the system. The rapidity distribution is found to differ with different clusterization systems. For the free nucleons, system is more thermalized with MSTB method while for the LMF's and IMF's fragments, the system are more thermalized with MST and MSTP method. This binding energy check will surely add valuable results in the understanding of nuclear stopping of nuclear matter.

3.6 Mass and charge distribution

In fig 3.5 and fig 3.6, the mass and charge distribution for the reaction $^{129}Xe_{54}$+$^{197}Au_{79}$ E=50MeV/nucleon and $^{36}Ar_{18}$+ $^{197}Au_{79}$ at E=50 MeV/nucleon at $\hat{b}$ = 0.6 using hard(left panel) and soft(right panel) equation of state.

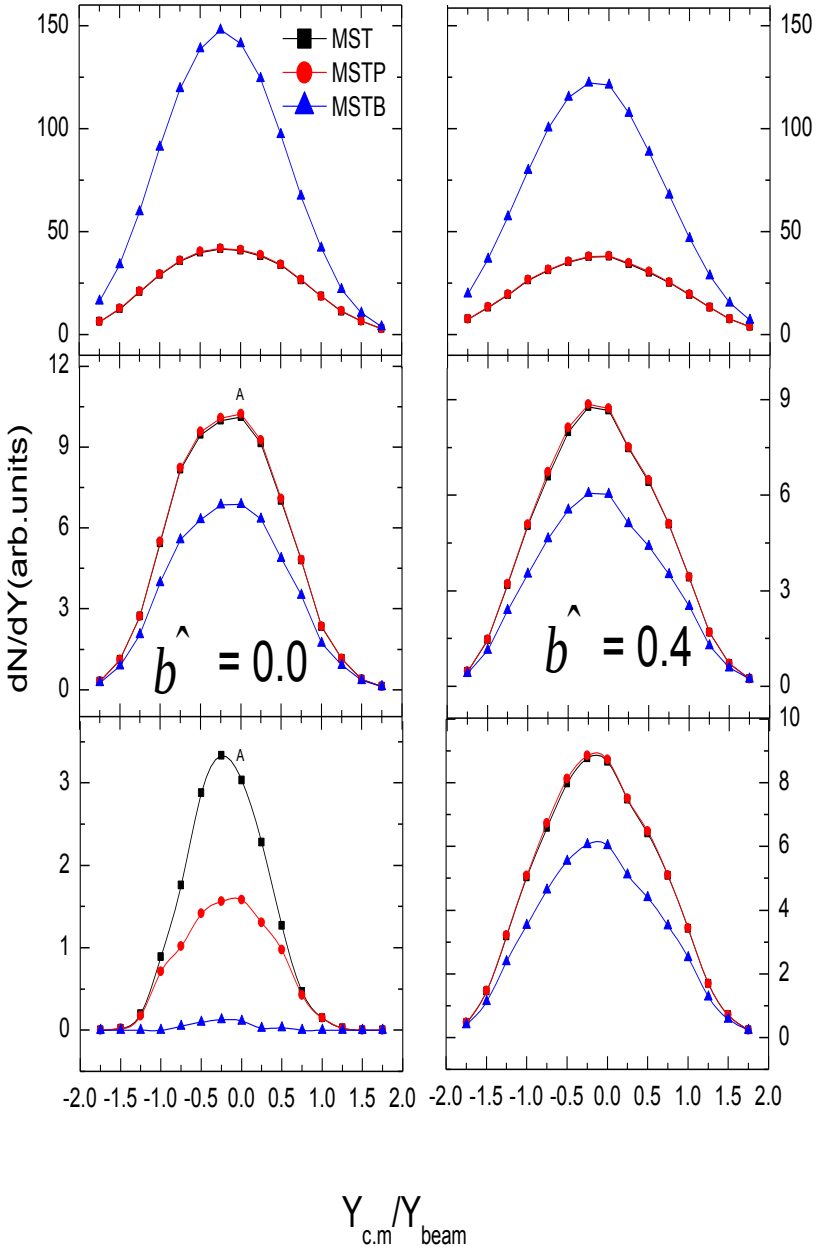

Fig3.4. The rapidity distribution for free nucleon, lmf, imf as a function of $Y_{c.m}/Y_{beam.}$

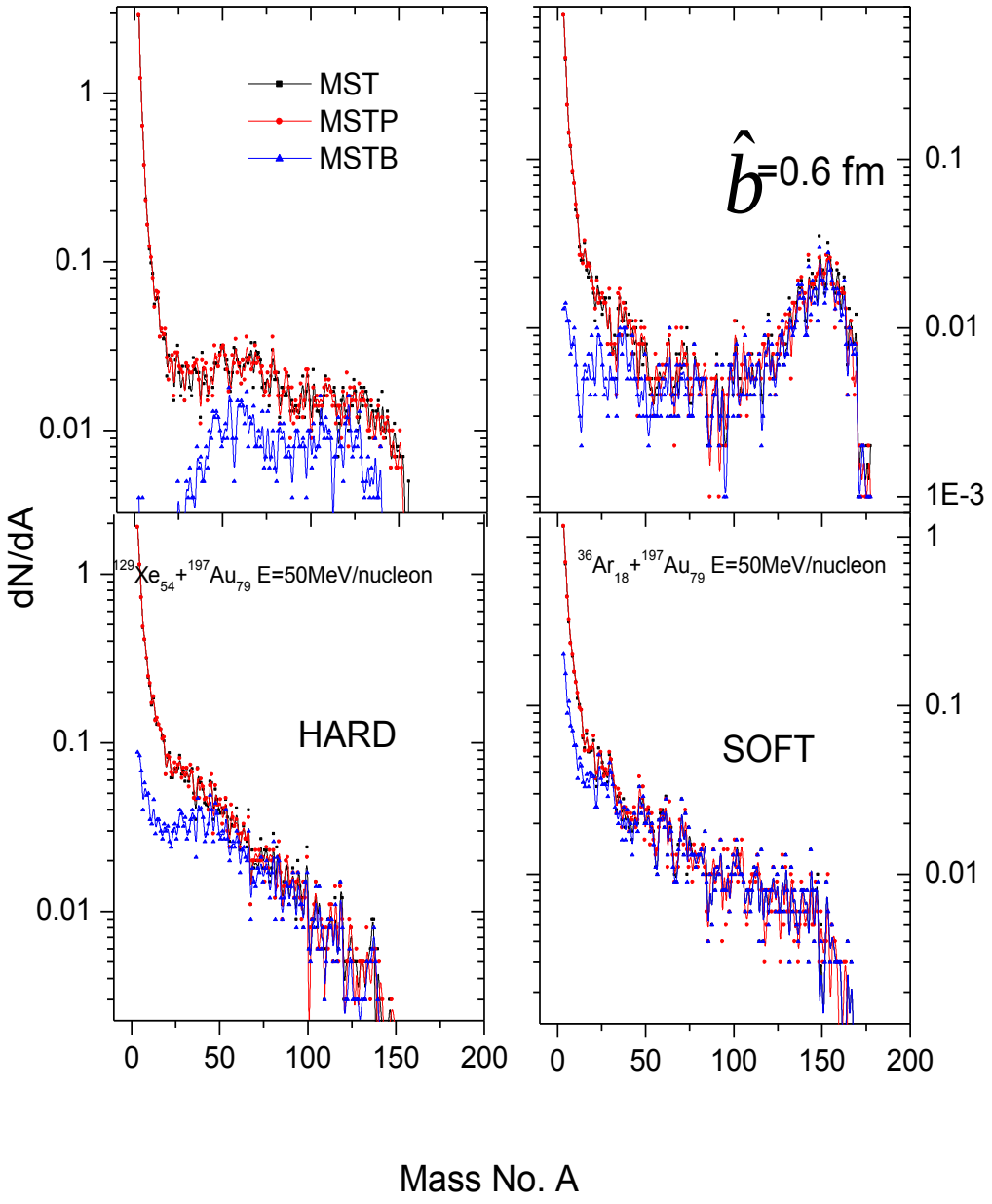

Fig 3.5 The mass yield d N/d A as a function of the mass of the fragments.

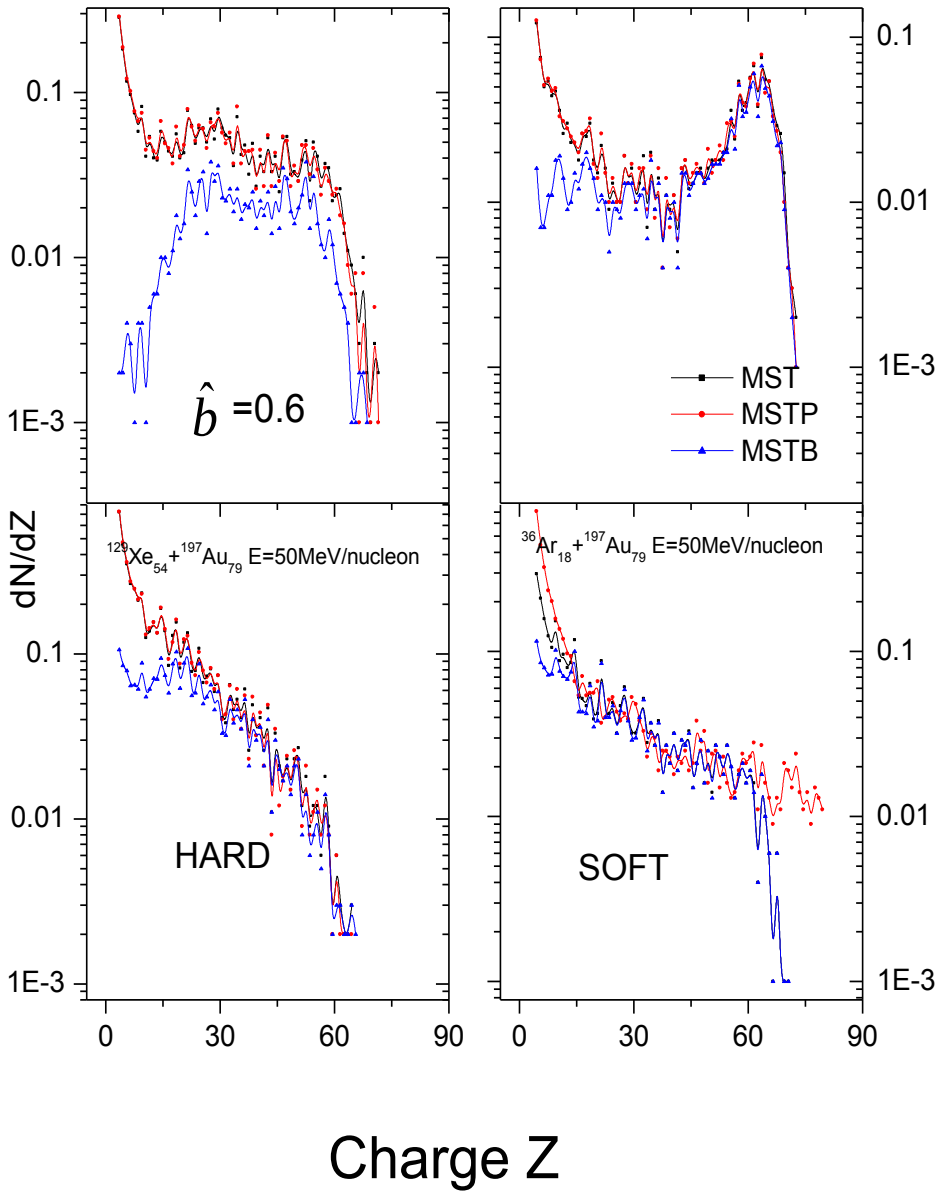

Fig 3.6 The charge distribution yield (d N /d Z) as a function of the charge of fragments.

In this fig. both the reactions $^{129}Xe_{54}+^{197}Au_{79}$ at E=50MeV/nucleon and $^{36}Ar_{18}+^{197}Au_{79}$ at E=50 MeV/nucleon, the hard equation of state is able to bring the bigger fragments.

One can see the bump in the graph when the asymmetry of the reactions is very high which leads to the production of the heavy fragments with hard equation of state. But in case of soft equation of state, we don't have heavy fragments for these two reactions.

One may be conclude that equation of state influence the production of the fragments and also effects the clusterization in the production of fragments.

3.7 Multiplicity as a function of impact parameter

To further check the effect of binding energy cut and momentum cut on light and heavy mass fragments. Fig 3.7 display the impact parameter dependence of final multiplicities of fragments with three different clusterization algorithms i.e. MST, MSTP and MSTB using hard equation of state. Here, we have displayed the multiplicity of free nucleons (A=1), LMF's ($2\leq A\leq 4$) and MMF's $5\leq A\leq 9$ for the reaction $^{36}Ar_{18}+^{197}Au_{79}$ at E=110MeV/nucleon. It is observed that the multiplicity of LMF's, free nucleons and IMF's go on decreasing as we move from central to peripheral collisions[9-10]. This is due to decrease in the participant zone with impact parameter. Moreover, the enhanced production of free particles is observed with MSTB and MSTP method as compared to MST, while opposite trend is observed for LMF's and MMF's. This is due to specified cut of 4 MeV in binding energy and 268 MeV/c in momentum speed for the fragment production in addition to the 4 fm cut in the simple MST method. This cut will make all the nucleons as free, which are loosely bond and lead to enhanced production of free particles. As discussed in the definition of MSTB and MSTP are more effective to study the fragment production.

3.8 Free nucleons as a function of impact parameter

Fig 3.8 shows the multiplicity of free nucleons as a function of scaled impact parameter for the two different reactions $^{129}Xe_{54}$ +$^{197}Au_{79}$ E=50MeV/nucleon and$^{36}Ar_{18}$+ $^{197}Au_{79}$ at different energies E=50, 80,110 MeV/nucleon. Here we have done the analysis with MST, MSTP and MSTB and compare with experimental findings. Although the results are not matching with experimental findings, but trend appear to be similar. This

may be due to the absence of filter in theoretical models. One can say that due to the binding energy cut in MSTB enhancement is observed in the production of free particles as compared to MST and MSTP method. This trend is supposed to be opposite for lighter and heavier fragments

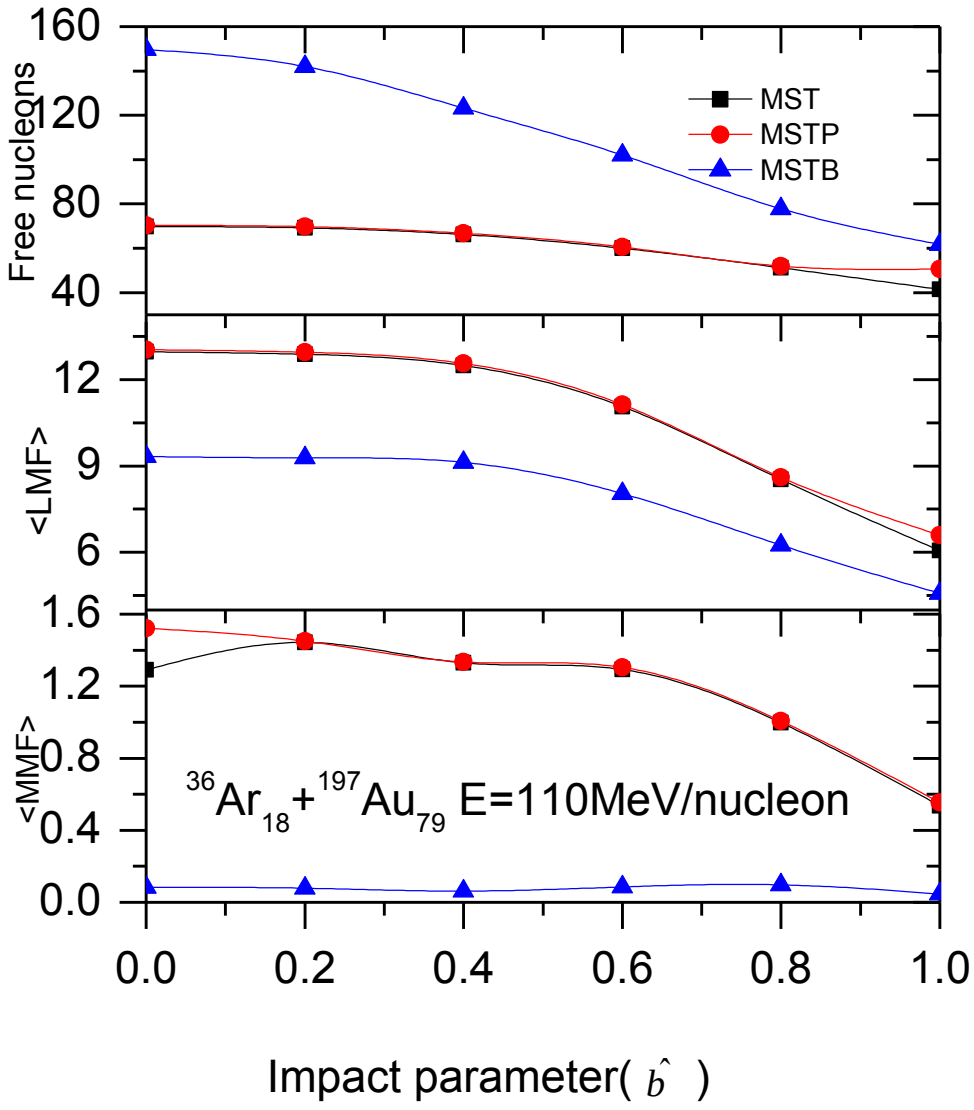

Fig 3.7 Multiplicity as a function of impact parameter.

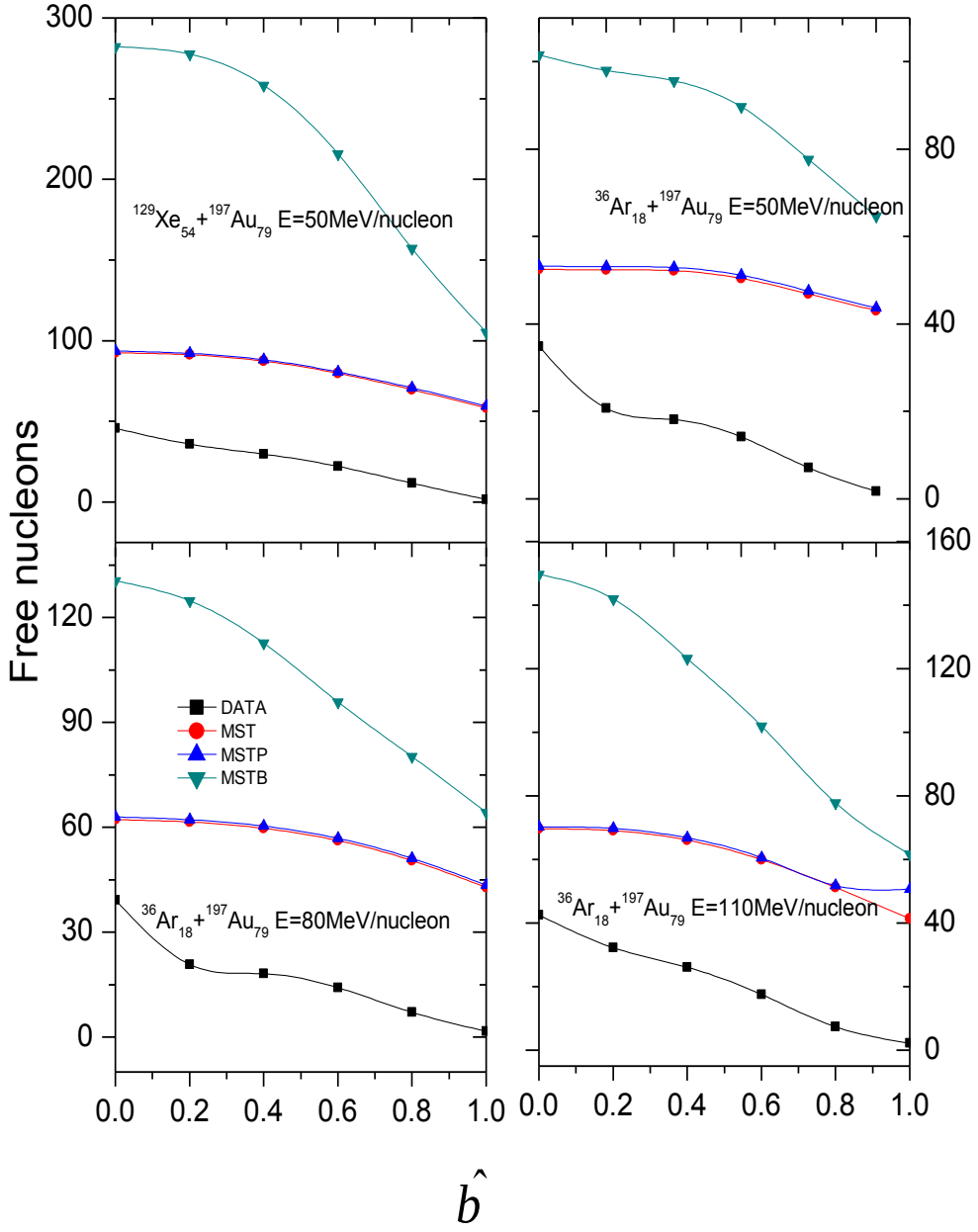

Fig: 3.8 scaled impact parameter as a function of free nucleons

3.9 Imf production dependence on projectile and target mass

The most prominent feature of the multifragment decay is the universality of the fragment and fragment charge correlation. The loss of memory of the entrance channel is an indication that equilibrium is attained prior to the fragmentation stage of the reaction. Here, we have shown the graph for the reaction for $^{129}Xe_{54}+^{197}Au_{79}$ at E=50MeV/nucleon. In fig 3.9, we have shown $<N_{imf}>$as a function of Z_{bound}. The quantity Z_{bound} is defined as sum of all atomic numbers Z_i of all projectile fragment with $Z_i \geq 2$. Here, in fig 3.9(a), 3.9(b), 3.9(c) and 3.9(d) we have displayed the effect of equation of state as well as the production of IMF's. All the panels i.e.3.9 (a), 3.9(b), 3.9(c) and 3.9(d) have similar trend. With increase in Z_{bound}, the production of IMF's is found to be decrease. Different values of Z_{bound} are devoting the different impact parameter. At the central collision, where whole of the matter acts as participant zone and production of IMF's is maximum. On the other hand, with increase in impact parameter, the participant zone decreases and spectator zone increases. The incident energy is too low to affect the spectator zone. After a certain impact parameter, the size of fragment becomes greater than the size of IMF's and hence decreases in IMF's with Z_{bound}.

On the other hand, the IMF's production is found to be enhanced with soft equation of state as compared to hard one. This is due to different compresibilties of soft (K=200 MeV) and hard (K=380 MeV) equation of state. If one compares (fig 3.9(b) and 3.9(c), 3.9(d) the fragment production in MST, MSTP and MSTB, then it is found to decrease to a significant level in MSTB as compared to MST and MSTP. This is due to binding energy cut of 4 MeV nucleon. This will naturally result in the enhanced production of free particles. These findings are shown in following figure.

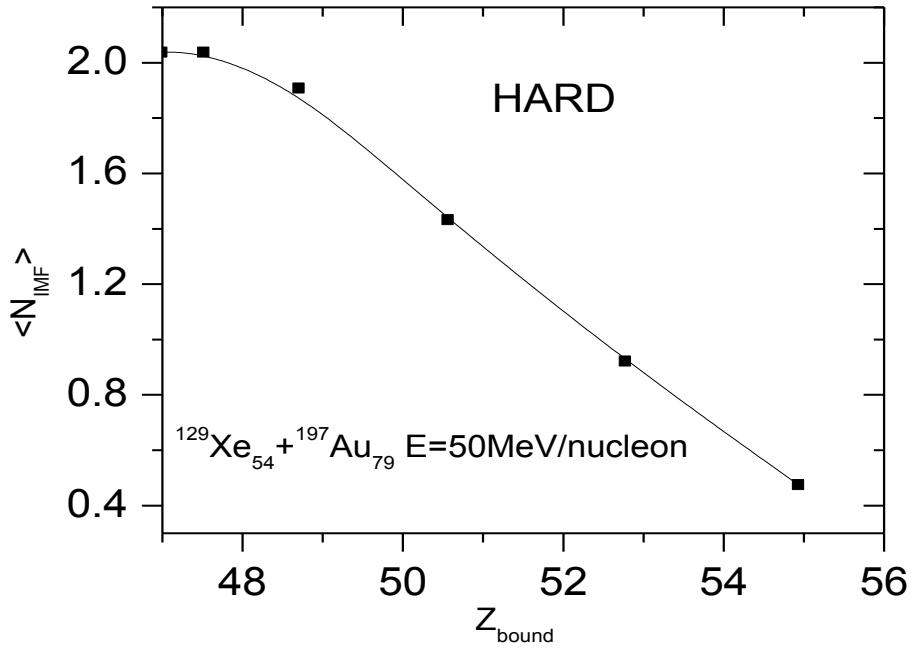

Fig 3.9(a). Multiplicity of IMF as a function of Z_{bound} for hard EOS.

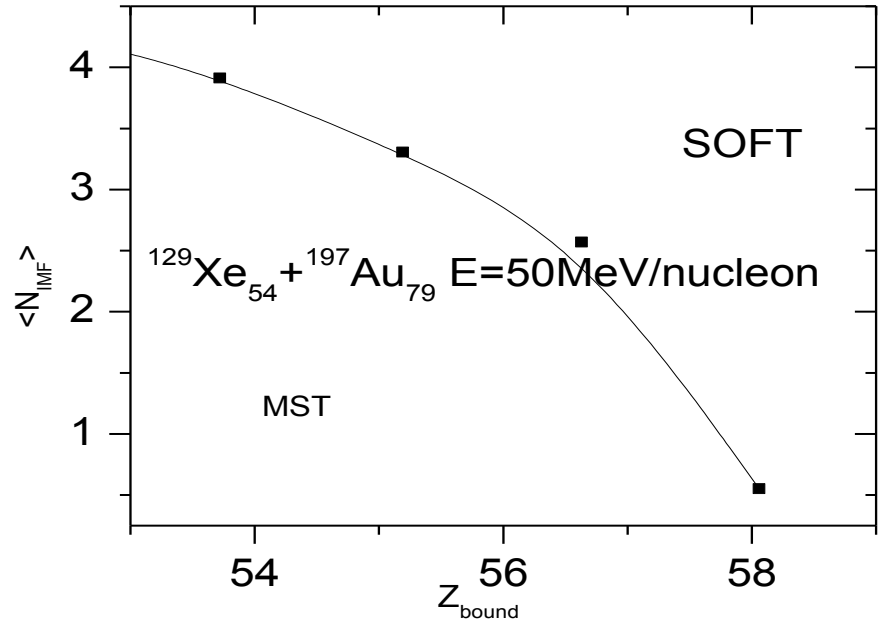

Fig 3.9(b). Multiplicity of IMF as a function of Z_{bound} for soft EOS.

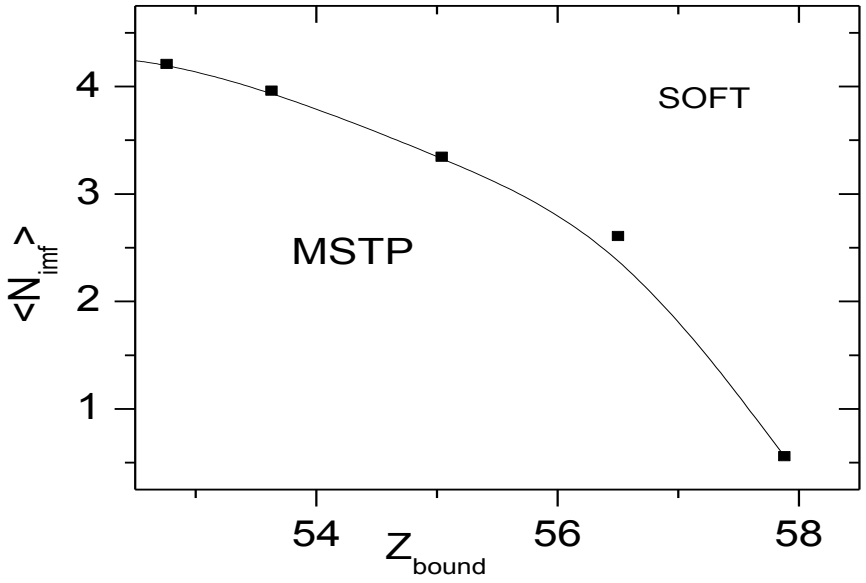

Fig 3.9(c). Multiplicity of IMF as a function of Z_{bound} for MSTP.

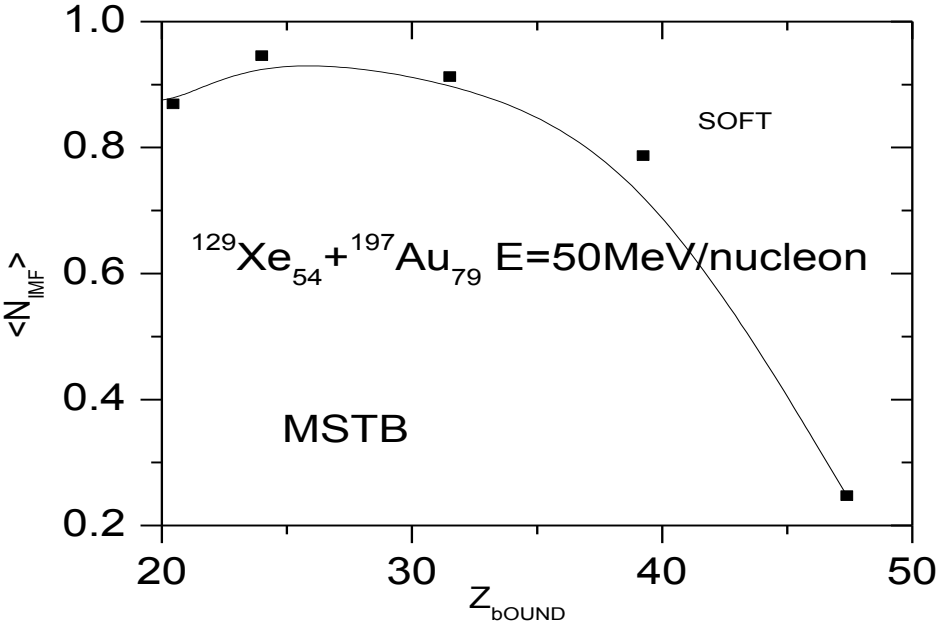

Fig 3.9(d). Multiplicity of IMF as a function of Z_{bound} for MSTB.

References

[1] Jaivir Singh and R. K. Puri Phys. Rev. C **62** 054602 (2000).

[2] J. Aichelin, Phys. Rep. **202**, 233 (1991).

[3] R. K. Puri and S. Kumar Phys. Rev **C 58,** 320 (1998); DAE Symposium On Nuclear Phys. 40 B, p. 152 (1997).

[4] A. Strachan and C. O. Dorso, Phys. Rev **C 56,** 995 (1997).

[5] S. Kumar and R. K. Puri Phys. Rev. C **58**, 320 (1998)

[6] S. Kumar and R. K. Puri Phys. Rev. C **58**, 2858 (1998)

[7] Jaivir Singh and R. K. Puri Nucl. Phys. **27** 2091 (2001).

[8] M. Begemann-Blaich *et.al.* Phys. Rev. C **48**, 610 (1993).

[9] S. Kumar and R. K. Puri Phys. Rev. C **60**, 054607 (1993)

[10] S. Kumar and R. K. Puri and J. Aichelin Phys. Rev. C **58**, 1618 (1987)

[11] R. K. Puri and S. Kumar Phys. Rev **C 57**, 2744 (1998), J. Singh, R. K. Puri, S.Kumar Phys. Rev **C 62**, 044617 (2000); ibid **65**, 024602 (2002).

Chapter 4

Summary

This thesis contains the theoretical description about the different clusterization algorithm in multifragmentation in intermediate energy heavy ion collisions. So in first chapter, we discuss about the heavy ion collisions and then their experimental and theoretical attempts in multifragmentation and then we discuss about the different primary and secondary models in multifragmentation

The various theoretical models are given in chapter 2. We have discussed in particular the IQMD model used for present study in different clusterization algorithms in multifragmentation.

In chapter 3, we discuss the effect of different clusterization algorithms as the multifragmentation by studying the multiplicity as a function of scaled impact parameter. The reactions of $^{129}Xe_{54}$ +$^{197}Au_{79}$ at E=50MeV/nucleon and $^{36}Ar_{18}$+ $^{197}Au_{79}$ at E=50,80,110 MeV/nucleon are simulated by varying the reaction geometry from central to peripheral . Our aim was to study the effect of different clusterization algorithms (MST, MSTP and MSTB) on multifragmentation. We concluded that MSTB and MSTP detect the fragments early as compared to MST.